Since January 2020 Elsevier has created a COVID-19 resource centre with free information in English and Mandarin on the novel coronavirus COVID-19. The COVID-19 resource centre is hosted on Elsevier Connect, the company's public news and information website.

Energy Nexus 6 (2022) 100080

Contents lists available at ScienceDirect

Energy Nexus

journal homepage: www.elsevier.com/locate/nexus

Plant-Based Natural Bioactive Compounds 2,4-Ditert-Butylphenolas: A Potential Candidates Against SARS-Cov-2019

Palanisamy Prakash[a,*], Kuppusamy Selvam[a], Ekambaram Gayathiri[b,*], Thangaraj Pratheep[c], Rengarajan Manivasagaperumal[d], Priya Kumaravel[e], Saravanan Balameena[f]

[a] Department of Botany, Periyar University, Periyar Palkalai Nagar, Salem 636011, Tamil Nadu, India.
[b] Department of Plant Biology and Plant Biotechnology, Guru Nanak College (Autonomous) Chennai 600 042
[c] Department of Biotechnology, Rathinam College of Arts and Science(Autonomous), Coimbatore 641021, Tamil Nadu, India
[d] Department of Botany, Thiru Kolanjiyapper Government Arts College, Virudhachalam, Cuddalore 606001, Tamil Nadu, India.
[e] Department of Biotechnology, St Joseph's College (Arts & Science), Kovur, Chennai, Tamil Nadu, India
[f] Department of Botany, Shri Sakthikailassh Women's college, Salem 636003, Tamil Nadu, India.

ARTICLE INFO

Keywords:
ADME/T
Network analysis
Docking
Molecular Dynamic
SARs-CoV

ABSTRACT

The novel coronavirus 2019 is spreading around the world and causing serious concern. However, there is limited information about novel coronavirus that hinders the design of effective drug. Bioactive compounds are rich source of chemo preventive ingredients. In our present research focuses on identifying and recognizing bioactive chemicals in *Lantana camara*, by evaluating their potential toward new coronaviruses and confirming the findings using molecular docking, ADMET, network analysis and dynamics investigations.. The spike protein receptor binding domain were docked with 25 identified compounds and 2,4-Ditertbutyl-phenol (-6.3kcal/mol) shows highest docking score, its interactions enhances the increase in binding and helps to identify the biological activity. The ADME/toxicity result shows that all the tested compounds can serve as inhibitors of the enzymes CYP1A2 and CYP2D6. In addition, Molecular dynamics simulations studies with reference inhibitors were carried out to test the stability. This study identifies the possible active molecules against the receptor binding domain of spike protein, which can be further exploited for the treatment of novel coronavirus 2019. The results of the toxicity risk for phytocompounds and their active derivatives showed a moderate to good drug score.

1. Introduction

The novel coronavirus 2019 is an active viral epidemic and increasingly outbreak globally [1]. The most specific symptoms of this disease are cough and sore throat [2–3]. The causative agent of this outbreak is the coronavirus, which belongs to group coronaviridae and order Nidovirales. The coronavirus is a large, enveloped, positive-stranded RNA virus with the largest genome ranging from 27 to 32 kb. They can be split into four genera: α, β, γ and δ. The α, β and δ coronavirus infect all humans, γ coronavirus infects avians [4]. In the viral assembly, membrane protein and enclosed protein are involved, while the spike protein settles at the entry of the virus into host cells. The spike is a central determinant of tissue tropism and viral host and a major inducer of host immune response. It first binds through its S1 subunit to a receptor on the outside of the host cell and through S2 subunit, fuses viral and host membranes. Two domains of S1 from various corona viruses identify an array of host receptors that are pivotal to the viral attachment. There are two structurally diverse conformations of the spike protein, prefusion and post-fusion, which is a crucial determinant of the coronavirus's pathogenicity [5].

The use of herbal medicine for therapeutic purposes should not be underrated, since so many herbal drugs have antiviral properties. Since conventional therapies have not been successful in suppressing SARS-CoV-2, well-known herbal medications with antiviral properties are now being employed as a supplementary therapy [6]. In contrast to synthetic antibiotics, the use of plants as natural, safe, accessible and economical materials for the treatment of bacterial infections has been expanding. In addition, as compared to chemical treatments, herbal medicines are

Abbreviations: ADME/T, Absorption Distribution Metabolism and Extraction Toxicity; PDB, Protein Data Bank; VS, Virtual Screening; GC-MS, Gas Chromatography-mass spectrography; 2D, Two Dimensional; 3D, Three dimensional; SAR, Specific Absorption Rate; MD, Molecular Dynamic; RMSD, Root mean square deviations; SSE, Secondary structure elements; RMSF, Root means square fluctuation; LC, Lantana camara; GO, Gene Ontology; BP, Biological process; MF, Molecular Function; SPC, Simple point charge.

* Corresponding authors:
E-mail addresses: drprakas2014@gmail.com (P. Prakash), gay3purush@gmail.com (E. Gayathiri).

https://doi.org/10.1016/j.nexus.2022.100080
Received 30 November 2021; Received in revised form 22 March 2022; Accepted 3 May 2022
Available online 12 May 2022

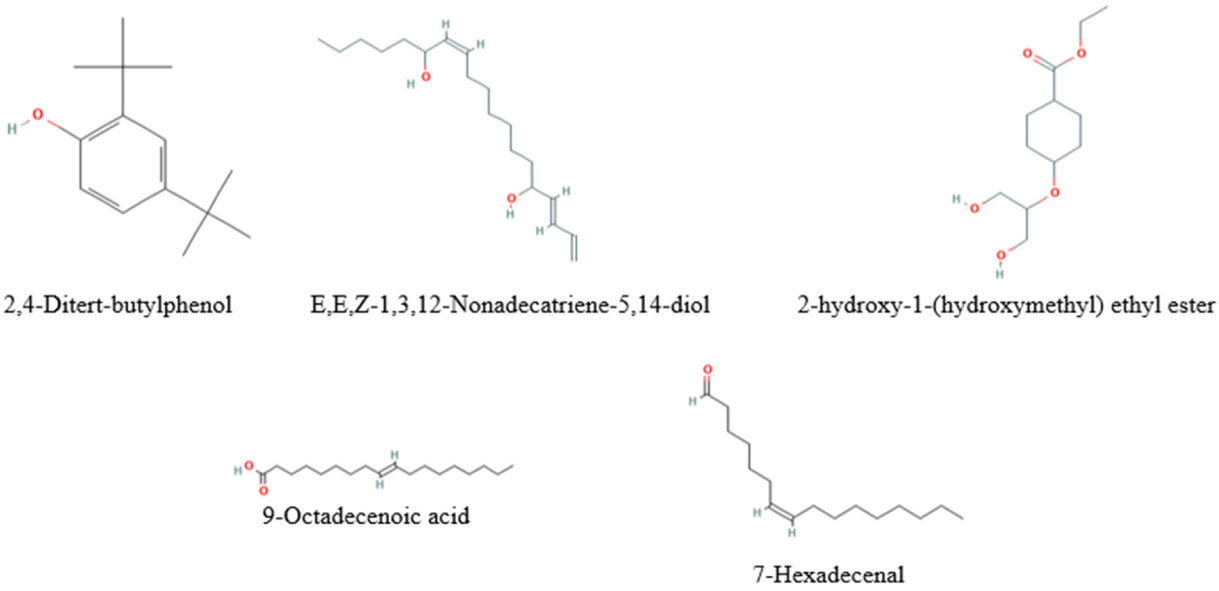

Fig. 1. Phytocompound compositions structure of *Lantana camara* leaf.

more popular among general public. Ayurvedic medicines gain immense recognition in the wake of COVID-19, it plays the powerful role against the corona virus. Currently, significant suggestions for potential phytocompounds act as inhibitor for various stages of tumor genesis and its inflammatory process and making them a promising therapeutic candidate [7]. Compared to modern medicine, herbal medicine contains life-saving properties with fewer side effects. Natural products are used for centuries as medicinal therapeutics, which are leading as a source of imperative remedies with pharmacognosy, dominating the improvement of rational drugs until the gradual development of target-based drugs over the last 50 years [8,9]. Different valuable herbal medicine can interfere with COVID-19 pathogenesis by inhibiting SARS-CoV-2 replication and entry to its host cells. Different phytocomponents are the most desirable herbal drink or fruit that can be introduced as effective adjuvant components in COVID-19 management and to reduce fever and cough as the most common complication of COVID-19 via anti-inflammatory effect. Computational methods are effective tool for developing drugs for targeted diseases. In our current research, we have selected phytocompounds from *Lantana camara* species, evaluate their effectiveness against to novel coronavirus 2019 through molecular docking, ADMET, network analysis and molecular dynamics.

2. Material and Methods

2.1. Plant material and Extraction

In the during August and September 2019, *Lantana camara* leaves were collected from Karuppur in Salem (Latitude **of** 39°34′18.41"N and a longitude of 75°28′1.71"W**),** Tamil Nadu, India. 100 gm of powdered leaf sample was extracted in a soxhlet apparatus for 8 hrs with solvent methanol [10]. The extract was filtered, pooled and solvent was evaporated in rotary evaporator (Heidolph, Germany) under reduced pressure at 40ºC, crude extract was stored at 4ºC in refrigerator for further analysis.

2.2. Identification of bioactive molecules in Lantana camara

The methanol leaf extract of *Lantana camara* species was done by GC-MS (Model; Agilent technologies 7890A) fitted with a fused silica capillary column of 30 m length, 0.25 mm diameter and 0.25 mm film thickness. An electron ionisation device with 70eV ionisation energy was employed for GC-MS detection. At a flow rate of 1 ml/min, helium gas (99.99 %) was employed as a carrier gas. Line temperatures were set at 220 and 200ºC degrees, respectively. After 2 min at 10°C/min, the oven temperature was scheduled to hold at 240°C for 6 min. In the splitless mode, 2 ml of water solution was manually introduced in the split ratio of 1:40 and with a mass scan of 50–600 amu. The GC-MS ran for a total of 35 minutes. Peak area normalization was used to calculate the relative concentration of each extract ingredient. Analysis of the plant extracts mass spectrum was carried out using the National Institute of Standards and Technology's library, which has more than 62,000 patterns. According to NIST library database, the compound's spectrum was evaluated towards the compound's spectrum (Fig. 1).

2.3. Preparation of protein and phytocompound structure

The spike protein receptor binding domain three-dimensional structure (ID: 6W41) retrieved from protein data bank, water molecules were removed and hydrogen molecules added into the structure. The phytocompounds 2,4-Ditert-butylphenol (ID: 7311), E,E,Z-1,3,12-Nonadecatriene-5,14-diol (ID: 5364768), 2-hydroxy-1-(hydroxymethyl) ethyl ester (ID: 59327317), 9-Octadecenoic acid (ID: 637517) and 7-Hexadecenal (ID: 5364438) retrieved from pubchem database.

2.4. Molecular docking studies

The molecular docking performed in Auto Dock 4.2, using Lamarckian genetic algorithm and the default protocols for docking a versatile ligand to a stiff protein. We ran docking calculations on the binding catalytic sites of each protein target. The 15 phytocompounds were docked to spike protein receptor binding domin and to determine the most probable and most energetically desired binding conformations. Using Autodock 4.2 [11], a grid box was employed to perform robust docking simulations. The e'completeness score for each protein-compound pair was 20. Active site encloses a docking array of 32 A3 with a grid spacing of 0.375 A. For 2,4-ditert-butylphenols, AutoDock Vina supplied a free energy binding hypothesis (in kcal/mol) that was used to calculate affinity scores (more negative value means greater binding affinity). A visual examination of the results using the Discovery studio DS Visualize 2.5 (http://www.dsbiovia.com/products) was carried out to verify the interactions.

Fig. 2. Three dimensional structure of spike protein receptor binding domine (ID: 6W41).

2.5. Drug Likeliness Prediction

"Lipinski drug philtres" (http:/www.scfbio-iitd.res.in/utility/Lipinskifilters.jsp) was used to forecast the ligand property. The Lipinski rule of five aims to differentiate drug-like and non-drug-like characteristics and forecasts a strong likelihood of molecular performance or failure attributable to drug likeliness. The Lipinski filters aims to prevent expensive late-stage preclinical and clinical errors in early preclinical evaluation.

2.6. SWISS- ADME/T

ADME and toxicity of the measured compounds was predicted using a large catalogue on the Swiss ADME web server (http://www.swissadme.ch/), and the server speculate with high precision on physiochemical assets, lipophilicity, water solubility, pharmacokinetics, drug-like and therapeutic properties.

2.7. Network pharmacology analysis

The network pharmacology analysis identifies the relationship between drug targets and investigate and characterize the small molecular inhibitor's multi-targeted existence. The network pharmacological method is commonly used to classify the future targets of organic products. A direct network interaction studies the relation between drug targets (https://string-db.org/). This site offers one potential biological data interaction for targeted organisms by creating multiple nodes and edges. The interaction between molecules and target proteins were subsequently chosen (docking scores were chosen to produce a target drug-target network virus) in which control points represent the molecules of the target protein virus and the properties of the network.

2.8. Molecular dynamics

The Desmond 2020.1 version of molecular dynamics simulations was used to analyze the structural integrity and stability of the receptor -ligand inclusion complex in an aqueous context. The apo -form spike receptor binding domain and the complex receptor binding domain of 2,4 Ditert butyl phenol have been explored. MD simulations were carried out using the force field of the OPLS-3e. The Simple point charge (SPC) [12] water model in an orthorhombic box with a ten-by-ten-by-ten-inch gap solved the systems. There were counter ions (Na+ and Cl-) in the salt solution that neutralized both processes and brought the salt concentration to 0.15 M. For 50,000 steps, the systems used the steepest descent strategy to reduce capacity. The systems were heated to 310K in a series of 100 ps NVT steps with protein backbone constraint using 100 kcal/mol constant forces. To balance the systems even further, NPT steps with a protein backbone constraint of 100 kcal/mol were used. It was maintained by the Nose-Hoover chain thermostat [13] and the Martyna-Tobias-Klein barostat [14]. At a wavelength of 10.0, the coulombic interactions with Van der Waals are terminated. To complete the NPT ensemble, MD simulations at 310K and 1.63 bar pressure for 50ns were run in the NPT ensemble using a 2 fs time step. Graphs and analyses were developed with Maestro and Xmgrace's Desmond simulation interaction diagram tool [15].

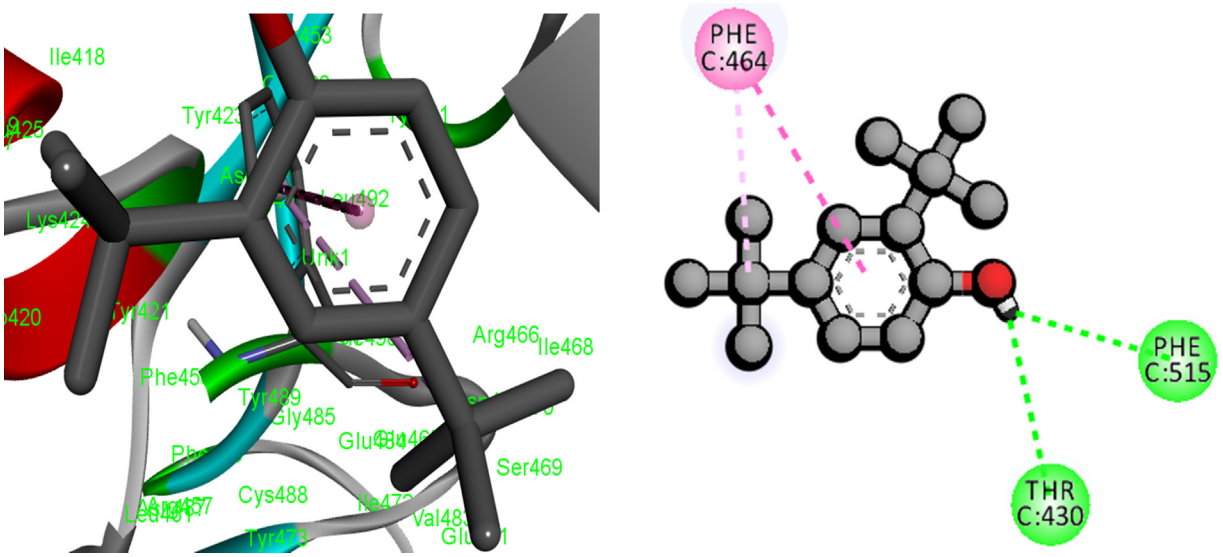

Fig. 3. Three dimensional structure of 2,4-Ditert-butylphenol interact with targeted protein.

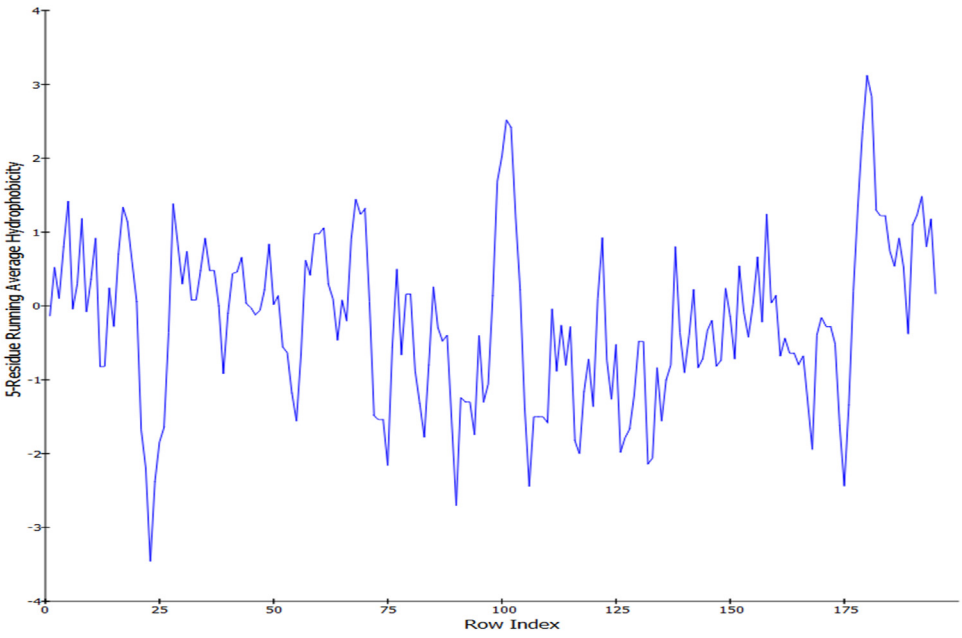

Fig. 4. Protein and ligand interactions plot.

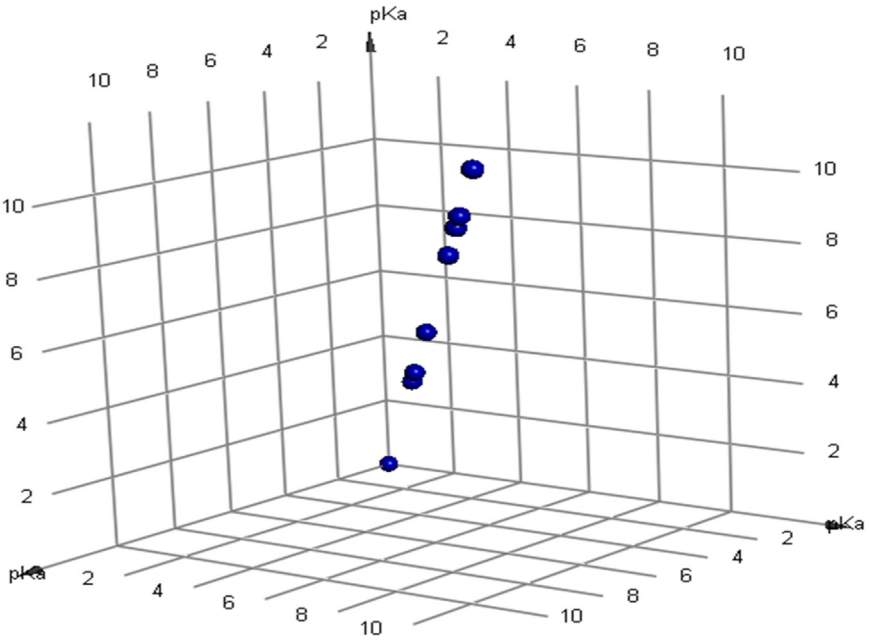

Fig. 5. Toxicity level for 2,4-Ditert-butylphenol interact with targeted ligand.

2.9. Binding free energy

PRODIGY-LIG (PROtein binding enerGY prediction - LIGands) was used to quantify the binding free energy (ΔG), which is a structure-based tool for predicting binding free energy in protein-ligand complexes [16]. To measure the binding free energy, it utilizes inter-molecular electrostatic energy, protein and ligand atomic contacts inside a 10.5 Å gap cutoff. By taking snapshots from the last 5 ns MD simulation trajectory, the binding free energy of the RBD and ligand complex was computed.

3. Results and Discussion

3.1. Molecular Docking analysis of bioactive compounds

Clinical trials were used to determine the effectiveness of drugs with the purpose of maximizing societal benefit while reducing time and expenditure in the area of drug development. Additionally, the docking effects were used to create the target network and investigate the pharmacological properties of desired selective antiviral inhibitors. Earlier studies indicated that ion channel is needed for the propagation of viruses; therefore, inhibitors targeting the E-protein can help to prevent the development of virus production [17]. Earlier reports indicated that it was active against SARS-CoV, despite the fact that antiviral activity had not been previously recognised. [18]. The study results executed for spike protein receptor binding domain (6W41) protein receptor with 25 compounds and the best five compounds was tabulated in Table 1. The binding energy of 2,4-Ditert-butylphenol, E,E,Z-1,3,12-Nonadecatriene-5,14-diol, 2-hydroxy-1-(hydroxymethyl) ethyl ester, 9-Octadecenoic acid and 7-Hexadecenal are -6.3, -6.1, -6.0 and -5.8 kcal/Mol respectively. (Figs. 2,3 and 4) In this protein-ligand interaction, the carbon and hydrogen interaction (Fig. 2) chain interacts well in the active pocket of the receptor, as shown in Figs. 3 and 4. The efficacy of a compound in patients with the disease proved that, the mentioned compound have more potentiality to treat, but there is a need to examine and determine the most suitable dose and route of administration.

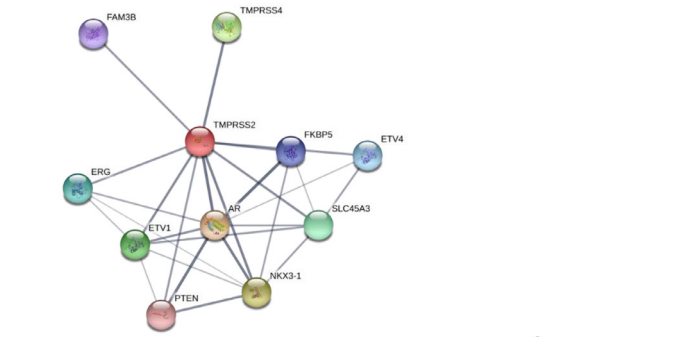

a

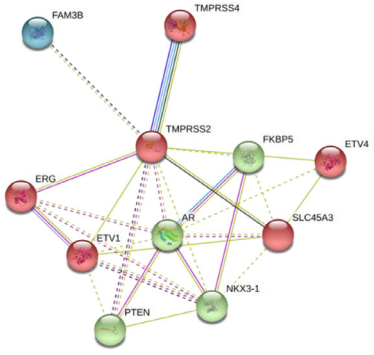

b

c

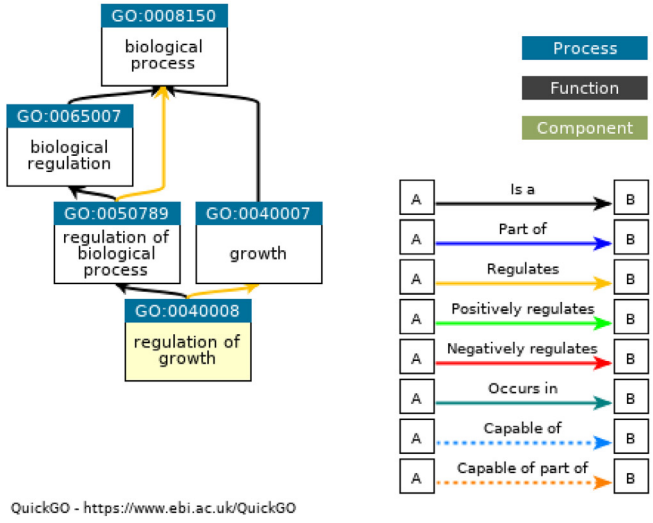

d

Fig. 6. (a-c) SAR-Cov19 target PPI network (27nodes 11edges) Protein-protein interaction network of targets related to viral protein. The colored nodes represent candidate proteins, and colored lines represent protein interaction High trust is described as a rating greater or equal to 0.839. TMRSS2, TMRSS4,AR,NKX3, and 1XQ8, as well as were two separate nodes with strong trust levels. (d) gene ontology (GO) enrichment analysis.

Table 1
Docking score results of 25 compounds with antiviral protein target

S.NO	NAME BIO ACTIVE COMPOUNDS	Binding energy in (6W41)kcal/mol
1	DODECANE	-5.0
2	Tetradecane	-5.2
3	2,4-DITERT-BUTYLPHENOL	-6.3
4	HEXATRIACONTANE	-4.9
5	EICOSANOIC ACID, METHYL ESTER	-5.6
6	n-Hexadecanoic acid	-5.0
7	Behenic alcohol	-5.3
8	Heneicosane	-5.4
9	9,12-OCTADECADIENOIC ACID (Z,Z)-, METHYL ESTER	-6.0
10	E,E,Z-1,3,12-Nonadecatriene-5,14-diol	-6.1
11	2-HEXADECEN-1-OL, 3,7,11,15-TETRAMETHYL-, [R-[R*,R*-(E)]]- 18 22.478 1602201 3.37 694357 3.67 9-Octadecenoic acid, (E)-	-5.4
12	Oleic Acid	-5.3
13	9-OCTADECENOIC ACID (Z)-	-5.8
14	Ethyl Oleate	-5.6
15	1-Heneicosanol	-5.5
16	Dotriacontane	-4.8
17	1-Heptacosanol	-5.3
18	7-Hexadecenal, (Z)-	-5.5
19	Hexadecanedinitrile	-1.2
20	Heptadecane	-5.5
21	2-Methylhexacosane	-5.5
22	Undec-10-ynoic acid, undec-2-en-1-yl ester	-1.8
23	1H-INDENE, 1-HEXADECYL-2,3-DIHYDRO-	-5.8
24	2-Methylhexacosane	-5.3
25	Hexadecanoic acid, 2-hydroxy-1-(hydroxymethyl)ethyl ester	-5.7

Finding a compound with the least toxicity or non-toxicity from all aspects is one of the key tasks of drug discovery [19,20]. Natural herbal drugs focus more on improving the immunity of the host as a whole, while allopathic drugs focus on the treatment of infectious agents [21].

3.2. Prediction of ADME/T studies

Many of these molecules have high gastrointestinal absorption, which enables them to be dose dependent internally and pass the most important drug discovery standard of decision-making. Both of the compounds would pass the blood-brain barrier permeability test. Consequently, they are known as the “fundamental drug delivery index”. The binding of the metabolic enzymes CYPD1A2, CYP2C19, CYP2C9, CYP2D6 and CYP3A4 can cause the toxicity of the compounds inside the body to degrade (Table 2a-2c). The 4-Ditertbutylphenol, 9-Octadecenoic acid (Z), 7-Hexadecenal, (Z), E, E, Z-1,3, 12-Nonadecatriene-5,14-diol and 2-hydroxy-1-(hydroxymethyl ethyl ester) compounds are unable to bind CYP2C19, whereas they can bind to CYP3A and CYP2C9. Therefore, the degradation of these key molecules within the body is highly likely, leading to the production of toxicity (Fig. 5). In a drug molecule, the bioavailability score of all the compounds is an indicator of high potential. Predicting the toxicity of the compounds under investigation is also a requisite this analysis. Various toxicity parameters, were tested for all the molecules. All these parameter values are in the region found for the successful molecule of the drug. This makes it really similar to molecules like narcotics (Table 2). The leading cause for confirming their efficacy is the bioactive compound

3.3. Network analysis of against the antiviral inhibitor’s targets

A PPI network (27 nodes and 11 edges) play a leading role in the pharmacological antiviral effects and enrich p value (0.05). FAM3B and TMPRSS4 are two targets that do not interact with other targets. The two distinct nodes with high confidence ratings were FKBP5 and ETV4, AR, NKX31, PTEN, and ERG, DRD2 (Fig. 6a-d).

Table 2
ADMET screening of selected compounds derivatives for *Lantana camara*.

S.No	Compounds name	Fraction unbound (Human)	BBB permeability	CNS Permeability	CYP2D6 substrate	CYP3A4 substrate	CYP1A2 inhibitor	CYP2C19 inhibitor	CYP2C9 inhibitor
1	Hexadecanoic acid, 2-hydroxy-1 (hydroxymethyl)ethyl ester	0.201	-0.263	-3.316	No	No	No	No	No
2	9-octadecenoic acid (Z)-	0.054	-0.142	-1.6	No	Yes	Yes	No	No
3	7-Hexadecenal, (Z)-	0.085	0.809	-1.511	No	Yes	Yes	No	No
4	E, E, Z-1,3,12-Nonadecatriene-5,14 diol	0.107	-0.426	-1.981	No	Yes	Yes	No	No
5	2,4-Ditert Butylphenol	0.044	0.478	-848	No	Yes	Yes	No	No

Table: 2a
ADMET screening of selected compounds derivative of *Lantana camara*

S.No	Compounds name	CYP2D6 inhibitor	CYP3A4 inhibitor	Total Clearance	Renal OCT2 substrate	AMES toxicity	Max. tolerated dose (human)	hERG I inhibitor	hERG II inhibitor
1	Hexadecanoic acid, 2-hydroxy-1 (hydroxymethyl)ethyl ester	Yes	No	2.004	No	No	0.332	No	No
2	9-octadecenoic acid (Z)-	No	No	1.936	No	No	1.936	No	No
3	7-Hexadecenal, (Z)-	No	No	1.884	No	No	0.013	No	No
4	E,E,Z-1,3,12-Nonadecatriene-5,14-diol	No	No	2.152	No	No	-0.096	No	No
5	2,4-Ditert-Butylphenol	No	No	0.759	No	No	0.42	No	No

Table 2b
ADMET Screening of selected compounds derivatives of *Lantana camara*

S.No	Compounds name	Oral Rat Acute Toxicity (LD50)	Oral Rat Chronic Toxicity (LOAEL)	Hepatotoxicity	Skin Sensitisation	T.*Pyriformis* toxixity	Minnow toxicity
1	Hexadecanoic acid, 2-hydroxy-1 (hydroxymethyl)ethyl ester	1.537	2.722	No	Yes	0.608	-0.487
2	9-octadecenoic acid (Z)-	1.429	3.187	Yes	Yes	0.701	-1.31
3	7-Hexadecenal, (Z)-	1.478	1.172	No	Yes	1.963	-1.07
4	E,E,Z-1,3,12-Nonadecatriene-5,14-diol	1.504	2.911	No	Yes	1.895	-0569
5	2,4-Ditert-Butylphenol	2.351	1.696	No	Yes	1.572	0.006

Table 2c
ADMET Screening of selected compounds derivatives.

S.No	Compound name	Water solubility	$CaCo_2$ permeability	Human Intestinal absorption	Skin Permeability	P-Glycoprotein substrate	P-glycoprotein I inhibitor	P-glycoprotein II inhibitor	VDss (human)
1	Hexadecanoic acid, 2-hydroxy-1 (hydroxymethyl)ethyl ester	-5.334	0.439	90.277	-2.797	No	Yes	No	-0.261
2	9-octadecenoic acid (Z)-	-5.862	1.57	92.329	-2.723	No	No	No	-0.587
3	7-Hexadecenal, (Z)-	-7.144	1.485	92.839	-2.398	No	No	No	0.458
4	E,E,Z-1,3,12-Nonadecatriene-5,14-diol	-6.14	1.586	90.725	-2.675	No	No	No	0.276
5	2,4-Ditert-Butylphenol	-3.924	1.666	92.034	-2.301	No	No	No	0.611

3.4. Molecular and pathway analysis

In order to further investigate the relevance of 27 targets, a gene ontology (GO) enrichment analysis was employed, which comprised of three parts: BP (Biological process), molecular feature, and biological process. As seen in the enrichment reports, a total of 433 results were provided for Gene ontology enrichment (0.893), including branch point prediction enrichment (59 and Molecular Functio 431). *Lantana camara* was mainly involved in four biological processes that included biological value management, androgen receptors, steroid hormone receptors which are ligand-activated transcription factors, that regulate eukaryotic gene expression The receptor-binding domain (RBD) in the spike protein is the most variable part of the coronavirus. It has antiviral property because it regulates four major MF: equivalent protein binding, protein homodimerization, and protein homodimerization function. The findings showed that, KEGG pathways analysis AR, TMBRSS2, and ETV1 were significantly enriched by pathways. The number of target charting pathways was higher than the viral ways (hsa05215, number=5 (hsa05202, number=5), (hsa05206, number=2), and the influenza virus (hsa05164, number=2).

3.5. Compound-targetpathway interaction analysis

The compound-target-pathway network has 27 nodes and 11 edges, with nodes conforming to the active molecules, goals or pathways and binding to the edges. Many *Lantana camara* compounds not only operate on the same target protein, but also on several target proteins, and several pathways act on a single compound, illustrating the synergistic impact of LC's "multiple components, multiple targets and multiple pathways. Finally, our research aims to demonstrate the detection of novel structures that have different structural properties with similar behavior with respect to the best energy level compounds 2,4-Ditert-butylphenol.

3.6. Molecular dynamics simulation

In order to test the stability of protein-ligand complex, one compound 2,4-Ditertbutyl-phenol derivative (-6.3 kcal/mol) with good binding energy was selected and subjected to molecular docking study and MD stimulation. After molecular simulation and refining, it is apparent that all complexes have been configured to the full extent and that the complex's total energy has also been stabilized for all structures with

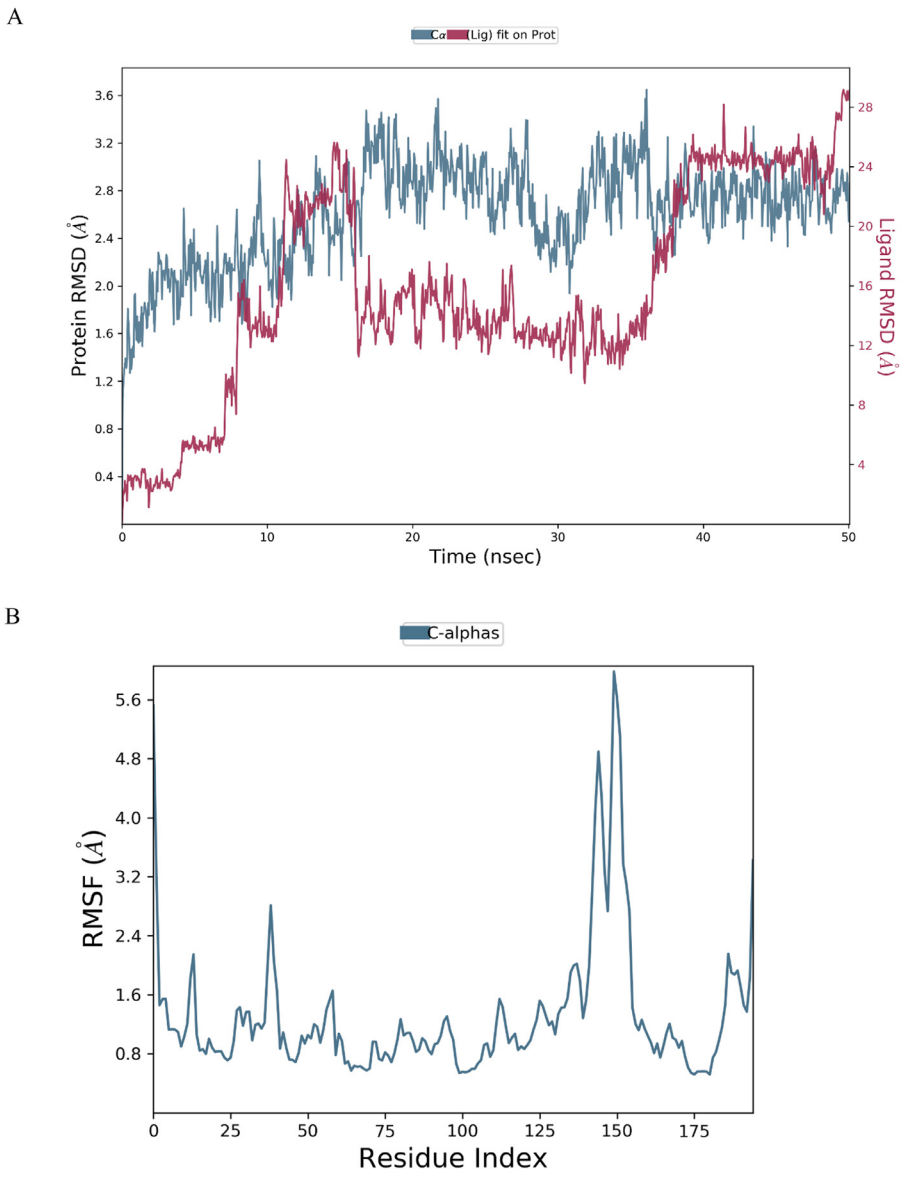

Fig. 7. Protein Cα atoms (A) time dependent RMSD plot, (B) RMSF plot over the 50 ns trajectory.

high RMSD performance in docking outcomes. The stability of protein validate by RMSD, used to examine the integrity of the ligand-protein complex during MD simulations. The C Alpha Atoms RMSD value of the apo and ligand bind form indicates all the most comparable partners across the 50 ns MD simulation. We also calculated C alpha RMSF to comply with local level stability, which measures the amino acid residue fluctuation at the time of MD simulation (Fig. 7, 8). For the apo and complex shape, no significant difference was found, which shows that ligand binding does not influence protein stability and reflects our RMSD findings. SSE comprising alpha-helical and beta-strand regions are correspondingly emphasized with red and blue backgrounds. SSEs regions are characterized by helices or strands that survive for simulation of over 70 percent and related patterns in verification of SSE binding affinity. A further time-dependent residue wise secondary structure chart has been determined for both structures and no major improvements have been found. This outcome confirms the analysis and experimental validation of SSEs.

3.7. Intermolecular Interactions

The ligand molecule forms links (PHEc515 THR c430) to the active amino acid site. Interaction of hydrogen with PHE515 in molecular docking at distances of 3.0, 4.96, Å and 3.0, respectively. The relationships between PHE.515 and THR (c430) did not differ significantly in the MD simulation (3.55 Å). For the inhibition of 6w41, this relationship is essential. Likewise, in molecular docking, the THR atom shapes hydrogen associations with PHE515 (2.5Å); during the MD simulation, this association is unchanged (5.00 Å). Amino acid residues that are part of the active site's structure interact with the ligand molecules (PHEc515) and THR (c430). In molecular docking, hydrogen interacts with PHE515 at wavelengths of 3.0, 4.96, and 3.0. The interactions between PHE.515 and THR (c430) were not particularly large in the MD simulation (3.55). This relationship is essential for the inhibition of 6w41. Similarly, the THR atom develops hydrogen associations with PHE515 (2.5Å) in molecular docking; and this relationship is unchanged during the MD simulation (5.00 Å).

The time-based intermolecular contacts were computed over the 50 ns MD simulation. The values over 1.0 suggest that there are residues forming several contacts with the ligand. During the simulation of 50 ns MD, up to 4 contacts are identified (Fig. 9). In biological systems, hydrogen bonds are one of the main components responsible for molecular interactions. Although many residues are involved in the creation of h-bonds, one of the main components responsible for molecular inter-

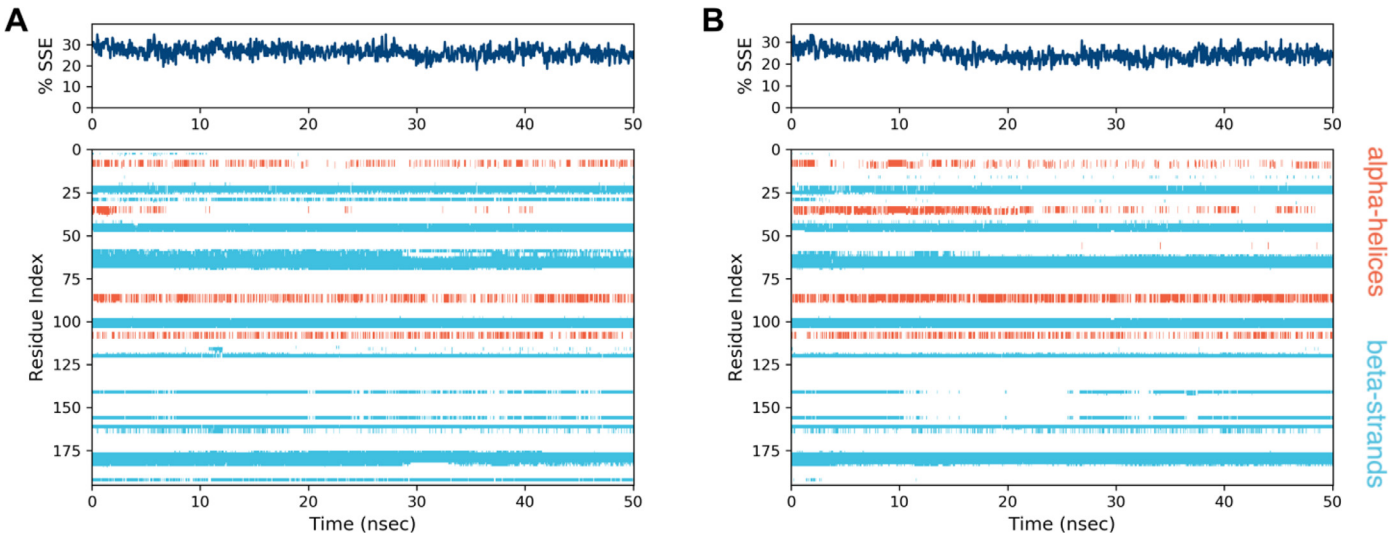

Fig. 8. Protein secondary structure prediction over the 50 ns MD simulation (A) Apo-protein, (B) ligand bound protein complex.

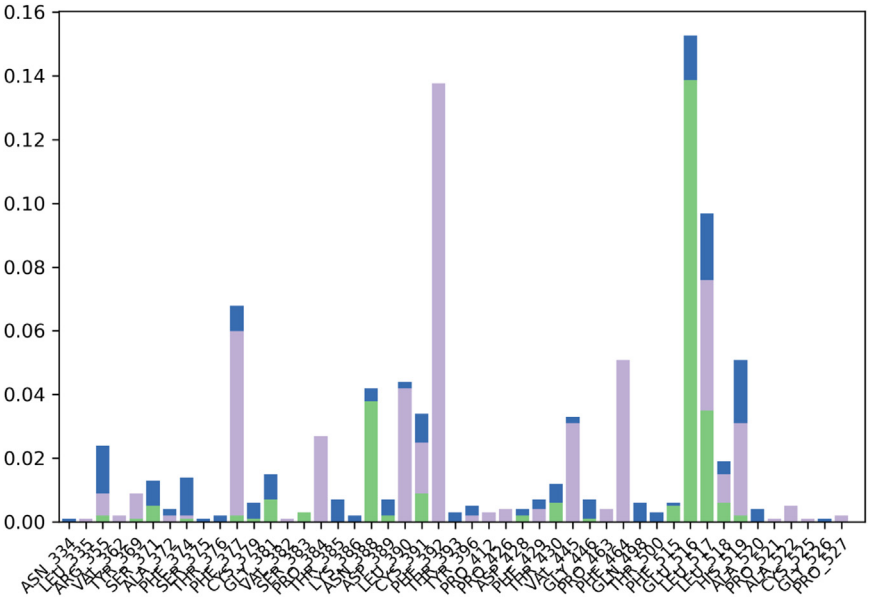

Fig. 9. Total number of contacts between protein and ligand analysis 50 ns.

actions in biological processes during MD simulation is hydrogen bonds. Changes in the secondary structures, which were in turn regulated by hydrogen bonds, were responsible for the protein-ligand interactions. The H bonds play a significant role in ligand binding throughout the course of the pathway to represent the encounters and experiences in the timeline. A critical body for determining their partnership is the mandatory free energy (ΔG) of the protein complex. The protein and ligand complex's binding free energies were calculated by taking 7 snapshots of the last 5 ns MD simulation trajectory and calculating it to be -92.3 kcal/mol using the PRODIGY-LIG method. According to available reports, several plant components can be used effectively as stimulators of non-specific immunity as well as for their curative properties to get rid of infective diseases [22–23]. In addition to host and pathogenic macromolecules, designed drugs based on structure and functions have high value in molecular medicine [24]. The most variable component of the coronavirus was classified as an imperative protein with considerable significance values based on the network topology analysis of the spike protein. The amino acids have been shown to be important for binding to ACE2 receptors and determining the host range of SARS-CoV-like viruses [25]. Similarly, our research [26] found a synergistic multi-effect result in the recommendation of TCM, CMs, and CMs, suggesting that anti-COVID-19 has more substantial benefits. An earlier article [27] discussed s "the neuroprotective properties of AP may be partially linked to its APP-BACE1-GSK3B signal axis regulation and irritation. At the needed site, the dynamic site filtrate was plotted, and it was determined that all of the extracts included the active portion of each target structure. The study of molecular structure has been the most important way to understand the molecular mechanism of drug activity today [28]. Although certain residues are involved in forming h-bonds, ASN388, GLU516, and LEU517 still have full occupancy during the MD simulation. Analysis has resulted in novel findings about the SARS-CoV cell entry mechanism [29]. Via two separate pathways: proteolytic cleavage of ACE2, which can facilitate viral uptake, and cleavage of coronavirus spike infection, TMPRSS2-human SARS coronavirus infection [30,31].

Molecular docking offers static poses in the binding pocket of a protein to express a stable complex of the most favored molecule conformations. The other primary structures required in maintaining a protein's stability are not visible in static pictures. These characteristics include the flexibility of residues and structural secondary components [32]. The

conformational changes resulting from the dynamic output of a protein can have an effect on its actual biological function [33–36]. Molecular docking and dynamics are the most important aspects of manipulating and exhibiting new bioactive compounds. [37]. Hydrogen bond is considered as a crucial type of interaction in drug discovery and development process, as of their strong influence on drug likeliness properties [38–39]. So finally our results work aims to demonstrate in identifying novel structures which are having similar structural feature with similar activity with respect to the compounds 2,4-Ditert-butylphenol that are shown best binding energy with the receptors spike protein respectively.

4. Conclusion

Phytochemicals derived from *Lantana camara* were docked with the SARS-CoV-2 6W41 virus to see whether it exhibits antiviral potential and also to search for the active components. Based on molecular docking, ADMET, network analysis, docking, and molecular dynamic research, we suggest that 2,4-Ditert-butylphenol might be employed as powerful inhibitors against coronavirus. The molecular docking, ADME/T and Lipinski's rule of five are fully filled with these inhibitors. Thus the interactions are important to inhibit the spike protein enzyme. The overall study will helpful do design a new potent inhibitor against enzyme. Due to the established history of 2,4-Ditert-butylphenol as a medication, the final suitable derivatives are quite likely to succeed in avoiding viral inhibitors infections. However, more in vitro and in vivo research are required to establish the drugs' antiviral efficacy against SARS-CoV-2019.

Author Contributions

PP, EG, and KS designed the research. PT performed the molecular docking, MD Simulations. PT did the MD analysis and binding free energy calculations. PP, EG, KS, PK, SB and PK wrote the article, and all authors reviewed the manuscript.

Declarations Ethics approval

Not applicable

Consent to participate

Not applicable

Consent for publication

Not applicable

Conflicts of Interest

The authors declare that they have no conflict of interest

Acknowledgments

We would like to express our gratitude to the Department of Botany at Periyar University in Salem for providing the services.

References

[1] P.X.L. Zhou, X.G. Yang, B. Wang, L. Hu, W. Zhang, H.D. Zhang, Chen A pneumonia outbreak associated with a new coronavirus of probable bat origin, Nature 579 (7798) (2020) 270–273.
[2] World Health Organization. Report, 2019: http://www.who.int/medicines/areas/traditional/definitions/en/
[3] Y. Wan, R. Graham, R.S. Baric, F. Li, An analysis based on decade-long structural studies of SARS 3, JVI, J Virol 29 (2020) Accepted Manuscript.
[4] J. Schaarschmidt Vangone, C. Geng P. Koukos, M.E. Trellet N. Citro, L. Xue, A.M.J.J. Bonvin, Large-scale prediction of binding affinity in protein-small ligand complexes: the PRODIGY-LIG web server, Bioinformatics 81 (2019).
[5] L. Fang, Structure, Function, and Evolution of Coronavirus Spike Proteins, Annu. Rev. Virol. 3 (1) (2016) 237–261, doi:10.1146/annurev-virology-110615-042301.
[6] L. Ang, Herbal medicine for the treatment of coronavirus disease 2019 (COVID-19): a systematic review and meta-analysis of randomized controlled trials, J. Clin. Med. 9 (5) (2020) 1583.
[7] D Shivakumar, J Williams, Y Wu, W Damm, J Shelley, W Sherman, Prediction of absolute solvation free energies using molecular dynamics free energy perturbation and the OPLS force field, J. Chem. Theory Comput. 6 (2010) 1509–1519.
[8] K Shirato, M Kawase, S. Matsuyama, Middle East respiratory syndrome coronavirus infection mediated by the transmembrane serine protease TMPRSS2, J. Virol. 87 (2013) 12552–12561.
[9] S.H. Shi, Y.P. Cai, X.J. Cai, X.Y. Zheng, D.S. Cao, F.Q. Ye, Z Xiang, A network pharmacology approach to understanding the mechanisms of action of traditional medicine: Bushenhuoxue formula for treatment of chronic kidney disease, PLoS One 9 (3) (2014).
[10] S Sasidharan, Y Chen, D Saravanan, K.M Sundram, L. Yoga, Latha. Extraction, isolation and characterization of bioactive compounds from plants' extracts, Afr. J. Tradit. Complement Altern Med. 8 (1) (2011) 01–10.
[11] S Release, Desmond Molecular Dynamics System, version 3.7, DE Shaw Research, Maestro- Desmond Interoperability Tools, New York, NY, 2014 2014 version, 3.
[12] Abraham, M. J, Murtola, T, Schulz, R, Smith, J. C, Hess, B., and Lindahl, E, GROMACS: High performance molecular simulations through multi-level parallelism from laptops to supercomputers, SoftwareX, 1-2, 19–25.
[13] S.K.T Reddy, V Reddy, V Kumari, S.H Basha, Molecular docking and dynamic simulation studies evidenced plausible immunotherapeutic anticancer property by Withaferin A targeting indoleamine 2, 3-dioxygenase, J. Biomol. Struct. Dyn 33 (2015) 2695–2709.
[14] S Perlman, J Netland, Coronavirus post-SARS: update on replication and pathogenesis, Nat. Rev. Microbiol. 7 (2009) 439–450.
[15] S.K. Pattanaya (2018). Alternative to antibiotics from herbal origin- outline of a comprehensive research project, Current personalized medicine. 16(1): 09-62.
[16] Nongluk Sriwilaijaroen, Yasuo Suzuki, Molecular basis of the structure and function of H1 hemagglutinin of influenza Virus, Epidemiol Immuno biol (4) (1986) 71.
[17] Mc Clenaghan Conor, Hanson Alex, Lee Sun-Joo, Colin G. Nichols, Coronavirus Proteins as Ion Channels: Current and Potential Research, Frontiers in Immunology 11 (2020) 2651, doi:10.3389/fimmu.2020.573339.
[18] S.D. Navaneethan, S. Aloudat, S. Singh, A systematic review of patient and health system characteristics associated with late referral in chronic kidney disease, BMC Nephrology 9 (1) (2008) 3.
[19] Z.W. Leung, Z.H. Jiang Cao, H. Zhou, Z. Zhang, W. Tang, Drug metabolism in drug discovery and development, Acta pharmaceutica Sinica. B 8 (5) (2018) 721–732, doi:10.1016/j.apsb.2018.04.003.
[20 Y.W Kam, Y Okumura, H Kido, LF Ng, R Bruzzone, R. Altmeyer, Cleavage of the SARS coronavirus spike glycoprotein by airway proteases enhances virus entry into human bronchial epithelial cells in vitro, PLOS ONE 4 (2009) 7870.
[21] Kalidas, Chandra, Pocket Depth: a new depth based algorithm for identification of ligand binding sites in proteins, Journal of Structural Biology 161 (2008) 31–42.
[22] M. Sivashanmugam John, S.K. Natarajan, V. Umashankar, Computational modeling of novel inhibitory peptides targeting proteoglycan like region of carbonic anhydrase IX and in vitro validation in HeLa cells, Journal of Biomolecular Structure & Dynamics 38 (7) (2020) 1995–2006, doi:10.1080/07391102.2019.1623075.
[23] Jaykant Vora, Shivani Patel, MohdAtharSonam Sinha, Mahesh T. Chhabria, C. Prakash, Jha & Neeta Shrivastava, Pharmacophore modeling, molecular docking and molecular dynamics simulation for screening and identifying anti-dengue phytocompounds, Journal of Biomolecular Structure and Dynamics (2019) 1726–1740.
[24] C Huthmacher, A. Hoppe, S. Bulik, H.G. Holzhütter, Antimalarial drug targets in Plasmodium falciparum predicted by stage-specific metabolic network analysis, BMC systems biology 4 (1) (2010) 120.
[25] L Gu, J Lu, Q Li, N Wu, L Zhang, H Li, X Zhang, A network-based analysis of key pharmacological pathways of Andrographis paniculata acting on Alzheimer's disease and experimental validation, Journal of Pharmacology and Experimental Therapeutics (251) (2020) 112488.
[26] V.Zoete Grosdidier, O. Michielin, SwissDock, a protein-small molecule docking web service based on EADock DSS, Nucleic Acids Res 39 (2011) 270–277.
[27] A.I Gray, J.O Igoli, R Edrada-Ebel, Natural products isolation in modern drug discovery programs, Natural Products Isolation (2012) 515–534.
[28] N. Ghamari, O Zarei, D Reiner, S Dastmalchi, H Stark, M Hamzeh-Mivehroud, Histamine, H3 receptor ligands by hybrid virtual screening, docking, molecular dynamics simulations, and investigation of their biological effects, Chem. Boil. Drug Des. 93 (2019) 832–843.
[29] J.H Fan, Y.Z Zuo, X.Q Shen, W.Y Gu, J.M Di, Development of an enzyme-linked immunosorbent assay for the monitoring and surveillance of antibodies to porcine epidemic diarrhea virus based on a recombinant membrane protein, Journal of virological methods 225 (2015) 90–94.
[30] L. Enjuanes, F Almazan, I. Sola, S Zuniga, Biochemical aspects of coronavirus replication and virus-host interaction, Annu. Rev. Microbiol. 60 (2006) 211–230.
[31] O. Michielin Daina, V. Zoete, Swiss ADME: a free web tool to evaluate pharmacokinetics, drug-likeness and medicinal chemistry friendliness of small molecules, Sci. Rep. 7 (2017) 42717.
[32] J Cohen, S.M. Opal, Powderly, Infectious diseases, 4thedn, Elsevier, UK, 2016 vol 1 and 2.
[33] K.J.Chow Bowers, D.E. Xu, H. Dror, R.O. Eastwood, M.P. Gregersen, B.A. Klepeis, J.L. Kolossvary, M.A. Moraes, F.D. Sacerdoti, J.K Salmon, Scalable Algorithms for Molecular Dynamics Simulations on Commodity Clusters, SC '06:, in: Proceedings of the 2006 ACM/IEEE Conference on Supercomputing, Tampa, FL, 2006, p. 43.
[34] S Boopathi, A.B.Kolandaivel Poma, P. Novel, Coronavirus structure, mechanism of

action, antiviral drug promises and rule out against its treatment, J. Biomolecular Structure and Dynamics. (2020) 1–10.

[35 V.K Bhardwaj, R Purohit, A new insight into protein-protein interactions and the effect of conformational alterations in PCNA, International Journal of Biological Macromolecules 148 (2020) (2020) 999–1009, doi:10.1016/j.ijbiomac.2020.01.212.

[36] S Bertram, I Glowacka, M.A.H. Muller, H Lavender, K Gnirss, Cleavage and activation of the severe acute respiratory syndrome coronavirus spike protein by human airway trypsin-like protease, J. Virol. 85 (133) (2011) 63–72.

[37] P.S.S Gupta, H.R Bhat, S Biswal, Computer-aided discovery of bis-indole derivatives as multi-target drugs against cancer and bacterial infections: DFT, docking, virtual screening, and molecular dynamics studies, Journal of Molecular Liquids (2018), doi:10.1016/j.molliq.2020.11437.

[38] D. Patel, M. Athar, P.C. Jha, Exploring ruthenium-based organometallic inhibitors against plasmodium calcium dependent kinase a combined ensemble docking, QM paramterization and molecular dynamics study funding sources, BioRxiv 2(PfCDPK2) (2020), doi:10.1101/2020.03.31.017541.

[39] P. Kovski, A. Kratzel, S. Steiner, Coronavirus biology and replication: implications for SARS-CoV-2, Nat. Rev. Microbiol. 19 (2021) 155–170, doi:10.1038/s41579-020-00468-6.